# Lawrence Berkeley National Laboratory

## Title

Templated self-assembly of one-dimensional CsPbX 3 perovskite nanocrystal superlattices

## Permalink

https://escholarship.org/uc/item/5qn1q706

## Journal

## ISSN

## Authors

Pan, Aizhao
Jurow, Matthew
Zhao, Yanrui
et al.

## Publication Date

## DOI

Peer reviewed

# Nanoscale

## COMMUNICATION

# Templated Self-Assembly of One-Dimensional CsPbX$_3$ Perovskite Nanocrystal Superlattices

Aizhao Pan,[a,b] Matthew Jurow,[b,c] Yanrui Zhao,[a] Fen Qiu,[b] Ya Liu,[c,d] Juan Yang,[c] Jeffrey J. Urban,[b] Ling He,*[a] Yi Liu*[b,c]

**Ordered self-assembled arrays or superstructures of nanocrystals (NCs) have attracted intense research interest due to their ability to translate valuable nanoscale properties to larger length scales. Numerous techniques have been explored to induce self-assembly into various superstructures. Here we investigated a simple kinetic approach to form self-assembled one-dimensional perovskite CsPbX$_3$ (X: halides) nanocrystal arrays templated inside a pod shaped inert lead sulfate (PbSO$_4$) scaffold. Both the solvent effects, and the self-assembly process and mechanism are systematically studied based on a uniform procedure developed to generate CsPbX$_3$ nanocrystal superlattices with different sizes and compositions. The formation of one-dimensional (1D) chains of NCs within a half-cylindrical pod of PbSO$_4$ reflects a balance between solvophobicity and solvophilicity of the components. By reducing the size of NCs, we successfully realized 2D superlattices with two or three rows of close-packed CsPbBr$_3$ NCs, in addition to single string-of-pearl type 1D assemblies. The superlattices can be assembled both inside and outside of the half-cylindrical shells by regulating reaction conditions. The self-assembly behavior is reminiscent of host-guest systems of organic molecular species where supramolecular recognition rules apply to give well-defined complexes. The current study opens a door for controlling self-assembled nanostructures of CsPbX$_3$ NCs, and provides an attainable platform for future optoelectronic devices.**

Colloidal nanoparticles (NPs) can be synthesized with precise control of composition, size and shape, yielding materials with vastly different physicochemical properties compared to their bulk counterparts.[1-5] Resultant properties can be further regulated by the hierarchical arrangement of individual nanoparticles, endowing self-assembled structures with collective properties distinct from

both individual NPs and bulk samples.[6-8] Self-assembled NP arrays including one, two, and three-dimensional superlattices, have attracted considerable attention in various research fields,[9-12] and created a wide range of applications for self-assembled nanostructures in functional nano-devices, including thermoelectrics, photovoltaics, catalysts, and sensors.[13-16]

Generally, the ascribed mechanism of solution phase self-assembly of NPs relies on the strong interactions between long-chain ligands on NP surfaces,[10, 16-21] or directional interactions between functional groups (polymers, DNA, inert nucleation materials),[9, 14, 19, 22] yielding equilibrium structures with a balance between inter-ligand and inter-particle interactions.[19, 23] However, the controllable assembly of inorganic nanocrystals into anisotropic structures still represents a significant challenge. Unlike the more controlled self-assembly systems such as organic molecular host-guest systems where an ensemble of molecular recognition principles, including induced fit, cooperativity, solvophobic interactions and solid state packing cooperate to give well-defined supramolecular structures, the assembly of inorganic nanoparticles may follow divergent kinetic pathways, resulting in inseparable mixtures or ill-defined structures [24, 25]. It would be highly desirable if the principles of molecular recognition could be applied in directing the kinetic and thermodynamic aspects of nanoparticle self-assembly.

AMX$_3$ type (A=cation, M=Pb, X=Cl, Br, I) lead halide-based perovskite nanocrystals (NCs) have attracted considerable research interest owing to their remarkable optical and physical properties.[3, 26-29] All inorganic CsPbX$_3$ (X=Cl, Br, I) NCs with various morphologies, sizes and optoelectronic characteristics can be synthesized by controlling the synthetic conditions and the composition of surfactant ligands during synthesis.[17, 30-33] Despite the substantial effort devoted to improving photoelectric properties by regulating structures, chemical composition, and size effects, only a handful of reports demonstrate controllable optoelectronic characteristics by engineering the secondary structure of CsPbX$_3$ NCs.[17, 34, 35] Both carboxylate and alkylammonium ligands are weakly bound to the NCs surface and susceptible to detachment, resulting in a loss of colloidal stability during polar solvent washes.[31] Self-assembled two-dimensional superstructures of CsPbBr$_3$ NCs can be created by

[a.] Department of Chemistry, School of Science, Xi'an Jiaotong University, Xianning West Road, 28, Xi'an, 710049, China, Email: heling@mail.xjtu.edu.cn
[b.] The Molecular Foundry, Lawrence Berkeley National Laboratory, Berkeley, California 94720, United States, Email: yliu@lbl.gov
[c.] Materials Sciences Division, Lawrence Berkeley National Laboratory, Berkeley, California 94720, United States
[d.] International Research Center for Renewable Energy, State Key Laboratory of Multiphase Flow in Power Engineering, Xi'an Jiaotong University, Xi'an, China
†Electronic Supplementary Information (ESI) available: Synthetic and self-assembly details, UV-Vis and PL spectra, PXRD, SEM, TEM and HR-TEM images.

taking advantage of this dynamic ligand environment to provide a natural driving force for spontaneous assembly processes.[17]
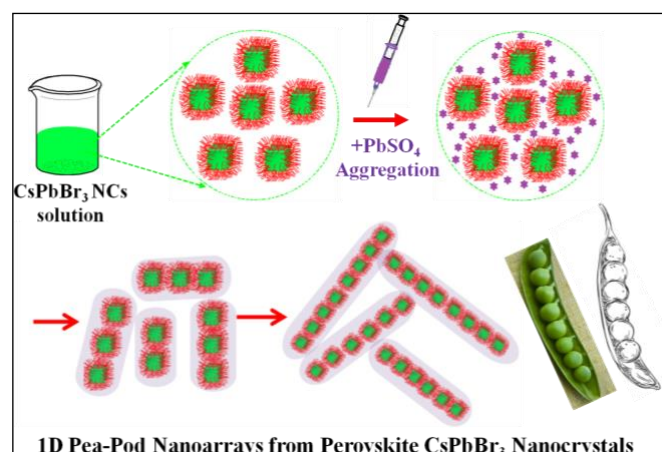


Scheme 1. Illustration of the formation process of the 1D superlattices of CsPbBr$_3$ NCs, green cubes, red wavy lines, purple dots and gray pod-like shapes represent CsPbBr$_3$ NCs, ligands on NCs, PbSO$_4$ clusters and PbSO$_4$ pods respectively

Methods to assemble one-dimensional superlattices of CsPbBr$_3$ NCs, however, have been very limited. Dong et al. pioneered a molecular cluster induced self-assembly method to grow 1D chains of nanoparticles, which is applicable to CsPbBr$_3$ NCs. We employed this approach to investigate the assembly process of CsPbBr$_3$ NCs, including exploring solvent dependence and size effect, and the formation process with time of 1D superlattices (Scheme 1). We have found that depending on the agitation mode of the assembly, i.e., with or without stirring/sonication of the mixture of the template and the NCs, different assembly structures can be obtained, which appears to be kinetic products with different thermodynamic stability. The 1D assembled outcome resonates with molecular recognition principles that are more commonly observed in organic supramolecular systems. A general procedure was developed to generate CsPbX$_3$ nanocrystal chains with different aspect ratios and compositions (CsPbX$_3$, X=Cl, Br or I), which may provide a valuable platform for the production of future optoelectronic devices, catalysts or sensors based on perovskite NCs.

The initial 1D assembly of perovskite NCs using clusters of lead sulfate was attempted following the protocol developed by Dong and co-workers.[34] Clusters of PbSO$_4$ were synthesized from PbCl$_2$, tetrabutylammonium hydrogen sulfate (TBAHS) and oleylamine (OAm) in CHCl$_3$, annotated as C-cluster throughout this discussion. The C-clusters incubated in hexane for 30 min were uniformly shaped lamellar ribbons of 38-45 nm wide (Fig. 1b). A solution of these clusters was mixed with a solution of 13 nm CsPbX$_3$ nanocubes in hexane and left undisturbed at room temperature to drive the self-assembled pea-pod-like superstructures (Fig. 1).[31, 34] TEM studies indicated that the self-assembly of nanocubes into 1D superlattice chains was induced within 30 min, with a majority of the NCs close-packed into straight linear chains in open pea-pod like PbSO$_4$ shells. The interparticle spacing in the superlattices is highly uniform (2.2 nm), consistent with surface ligand mediated packing.[31]
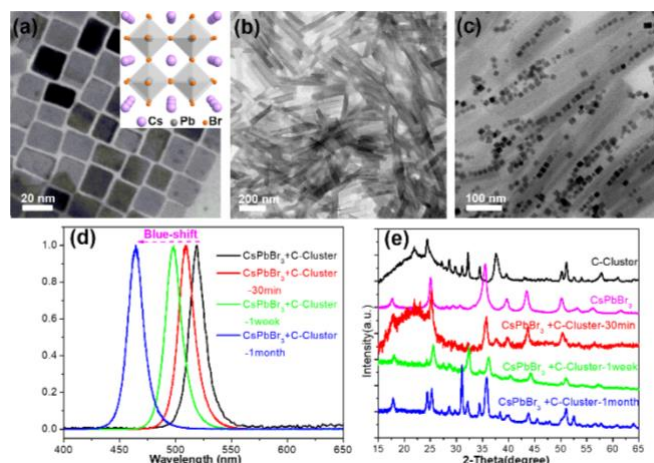


Fig. 1. (a) TEM image of typical CsPbBr$_3$ NCs with crystal structure image inset. (b) TEM images of pure PbSO$_4$ clusters in hexane from chloroform after 30 min incubation. (c) TEM image of 1D self-assembled superlattices of CsPbBr$_3$ NCs induced by 30 min incubation with clusters of PbSO$_4$ in chloroform. (d) PL emission spectra of the same 1D self-assembled superlattices incubated for times up to one month. (e) PXRD pattern (Co K alpha) of PbSO$_4$ clusters, free CsPbBr$_3$ NCs and the self-assembled superlattices at various times.

### Kinetic assembly behavior

The dependence of the self-assembly process into 1D superlattices was correlated with time by examining aliquots of the mixed samples with TEM and SEM. Upon addition of a solution of PbSO$_4$ clusters to the NCs solution, random mixtures of NCs and PbSO$_4$ clusters were observed (Fig. S1b). After 5 min incubation, partially assembled 1D structures with short chains of several NCs embedded in partially-filled PbSO$_4$ clusters were observed, together with many NCs randomly located outside the cluster barrier (Fig. S1c). The 1D chains continuously grew over time and reached an equilibrium state after 30 min incubation (Fig. S1g and f). The basic formation process is illustrated in Scheme 1.

When the PbSO$_4$ clusters were incubated in hexane in the absence of CsPbBr$_3$ nanocubes under identical conditions for 30 min, only uniform lamellar ribbons (38-45 nm wide) were observed (Fig. S1a, d and e).[34] In the co-assembled pea-pod superstructure, the formation of the 1D chains of NCs also stimulated the curving of the PbSO$_4$ shell to form half closed wrap around the NCs[34], an "induced fit" behavior that resembles biological enzyme-substrate recognitions.

Photoluminescence (PL) studies revealed a time-dependent hypsochromic shift for the PL emission peak. After 30 minutes incubation, the resulting 1D pea-pod superstructure displayed an emission maximum at 495 nm, 15 nm blue shifted from the initial peak wavelength of the free NCs (Fig. 1d). This trend continued for as long as a month in solution (Fig. S2). The blue shift was consistent with the exchange of bromides in the perovskite NCs with external chlorides. The PbCl$_2$ precursor used in the synthesis of the PbSO$_4$ clusters was not the source of chloride, as similar blue shift was also observed in parallel control experiments where PbCl$_2$ was replaced with PbBr$_2$ or PbI$_2$ precursors (Fig. S3). More convincing evidence comes from the control experiment from

which exposure of a CHCl$_3$ solution of neat CsPbBr$_3$ NCs to UV-vis light irradiation displayed similar blue shift (Fig. S4). This solvent-dependent halide exchange is also consistent with a recent study,[36] confirming that the CHCl$_3$ solvent is the source of the exchanging chlorides and is responsible for the spectroscopic shifts.

The powder X-ray diffractogram (PXRD) of the self-assembled 1D superlattices showed peaks at 2$\vartheta$=17.6, 25.1, 35.6, 39.6, 43.5, 50.2, 53.2 and 56.2°, consistent with the orthorhombic CsPbBr$_3$ crystal phase (JCPDF #01-072-7929) (Fig. 1e).[31] A slight shift of the diffraction peaks toward larger angles is evident over time, corroborating the proposed chloride exchange process. The TEM images of the self-assembled samples after 1 month revealed the rupture of the 1D structure and the formation of large and irregular NCs or nanoplatelets (NPLs), possibly due to degradation and restructuring influenced by anion-exchange and excess oleylamine ligands from cluster (Fig. S5).[30, 37]

### Solvent effects

The stability of the self-assembled superstructures is strongly solvent-dependent. The 1D superlattices can disassociate into random mixtures of NCs and PbSO$_4$ clusters if the mixture is dispersed in solvents such as CHCl$_3$ and THF, which can be re-assembled by the addition of hexane. This reversibility is driven by the solubility of the inorganic led precursors in CHCl$_3$ or THF, which contrasts with their nucleation into pods in poor solvents. The transformation in hexane of PbSO$_4$ clusters from flat ribbons into half-tubular shells suggests that the co-assembly with CsPbBr$_3$ NCs is energetically more favorable, which may be attributed to the screening of unfavorable interactions between the clusters and hexane by the favorable hexane-CsPbBr$_3$ NC interactions. In this way, the evolution of 1D chains of nanocrystals within a half-cylindrical shell of PbSO$_4$ reflects a balance between solvophobicity and solvophilicity of the components.





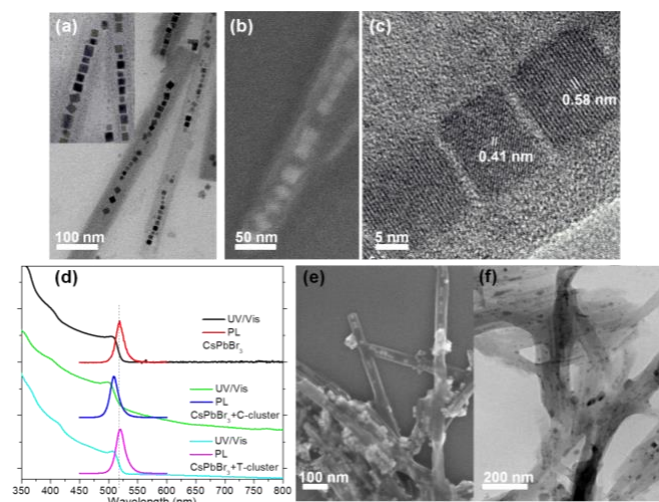Fig. 2. (a) TEM, (b) SEM and (c) HR-TEM images of the 1D self-assembled superlattices of CsPbBr$_3$ NCs formed in PbSO$_4$ shells in THF (T-cluster). (d) Optical absorption and PL emission spectra of comparing arrays induced by clusters of PbSO$_4$ in CHCl$_3$ (C-cluster) and THF (T-cluster) over 30min. (e) SEM and (f) TEM images of the superlattices assembled from T-cluster after 1 month.

Since the CHCl$_3$ solvent adopted in the original method for the lead cluster synthesis results in anion exchange in the perovskite NCs, a non-halogenated replacement was employed to maintain material stability during explorations of the self-assembly process. To this end, THF was used to synthesize analogous lead-based inorganic precursors, labelled here as T-cluster. Close-packed linear chains of CsPbBr$_3$ NCs (13 nm) embedded in a uniform half-cylindrical shell (35-40 nm wide), similar to these induced by C-clusters, can be obtained (Fig. 2a and b) by incubating with T-clusters. High-magnification TEM (Fig. 2c) confirmed the crystal lattice of CsPbBr$_3$ NCs in the 1D structure: the $d$ spacings of 5.8 Å and 4.1 Å can be clearly identified, corresponding to the (001) and (110) crystal lattice planes, respectively. In clear contrast to assemblies from C-clusters, with a time-dependent hypsochromic shift, Fig. 2d illustrates that the PL peak of assemblies from T-clusters present no changes after 30 min, indicating little to no damage to the crystal structures in THF. It is worth noting that the photoluminescence quantum yield (PLQY) of the CsPbBr$_3$ assemblies was vey high, ca. 70%, only slightly lower than the free NCs (ca. 74%), possible attributed to the enhanced interparticle interactions.

Considering the critical importance of environmental stability in most potential long-term applications, the effect of temperature before and after self-assembly was examined. Stability to ambient conditions was evaluated by storing at room temperature and relative humidity(RH) of 40-60%, subsequent the PL intensity of the assemblies were much higher than free NCs after 1 month of exposure. Moreover, neither the PL peak nor the PXRD pattern (orthorhombic phase, JCPDF#01-072-7929) displayed any notable changes even after 1 month of incubation (Fig. S6a and b). The TEM and SEM studies of the samples incubated for a month revealed that the majority retained the 1D pea-pod feature, with only small portions of 1D shells decorated with external NCs (Fig. 2e and f). Beyond that, temperature-dependent stability testing indicated that the assemblies present slightly improved thermal stability relative to the free NCs. After contact with water for 30 seconds, the CsPbBr$_3$ assemblies continued to emit weakly while films of free NCs were completely quenched (Figure S6). These stability improvements are possibly attributed to the protective barrier of the cluster shell and help prevent the total degradation of the contained CsPbBr$_3$ assemblies.
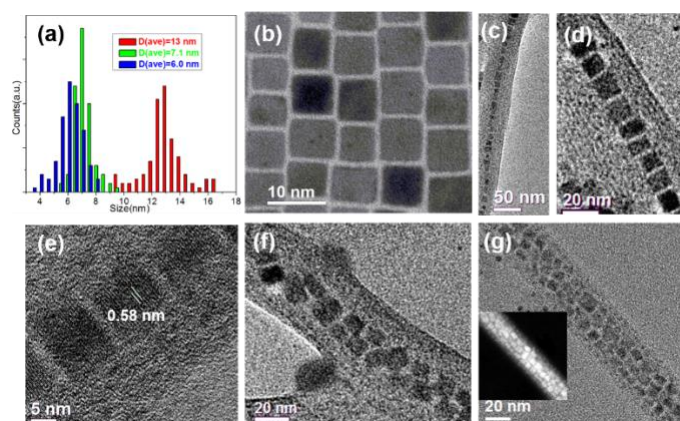
### Multidimensional Lattices



Fig. 3. (a) Histogram of CsPbBr$_3$ NCs sizes from TEM images. (b) TEM

image of CsPbBr₃ NCs (7.1nm). (c/d, f, and g) TEM images of the single line, double line and multi-line self-assembled superlattices of CsPbBr₃ NCs with T-PbSO₄ shells. (e) HR-TEM of the self-assembled structure of CsPbBr₃ NCs. Insets in (g) is the STEM image of a multi-line self-assembled superlattice of CsPbBr₃ NCs.

This PbSO₄ cluster-mediated self-assembly is broadly applicable to CsPbBr₃ NCs with different sizes and aspect ratios. The width of the T-cluster shelling remains constant between 38-45 nm (Fig. S7). Using this static geometry, the self-assembled superlattices can be regulated by using different sized CsPbBr₃ NCs (6.1-13 nm, Fig. 3a). Single and double file lines of close-packed CsPbBr₃ NC nanostructures with average interparticle distance of 2.2 nm were obtained using 7.1 nm CsPbBr₃ nanocubes (Fig. 3). The linear morphology and crystallinity were confirmed by HR-TEM, with clearly observable crystal lattice planes of (001) (d spacing: 5.8 Å, Fig. 3e).

Self-assembled chains with three rows of close-packed CsPbBr₃ NCs were realized when smaller CsPbBr₃ NCs (6.1 nm) were employed (Fig. 3g). The multi-line assembly within the certain diameter of the pea-pod structures is reminiscent of the tight-fit characteristics in molecular host-guest systems,[38-41] and is consistent with the increasing capacity of the host towards the NCs guests as the size of the guests scales down. Such assembly is presumably stabilized by the increased overall interactions between surface ligands and the T-clusters, as the smaller CsPbBr₃ NCs have a larger surface area and thus more surface ligands are exposed to the inner shell.
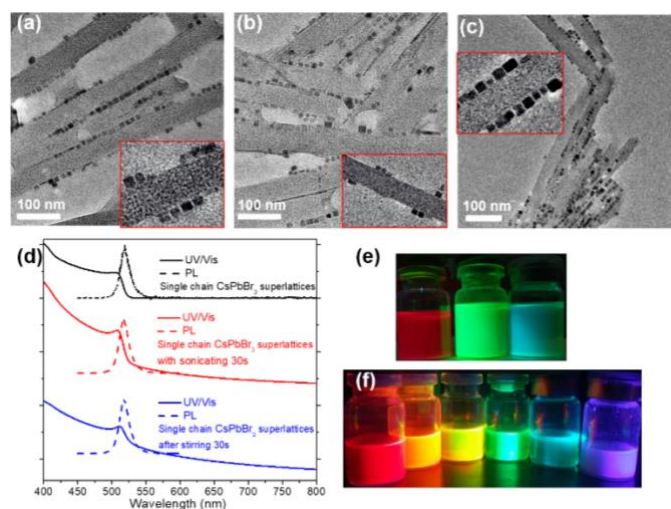
### Mechanical stimulation induced assembly behaviour



Fig. 4. (a) TEM image of single chain superlattices after sonicating for 30s. (b) TEM images of the self-assembly process of CsPbBr₃ NCs with T-PbSO₄ clusters under sonication for 30 min. (c) TEM image of single chain superlattices after stirring for 30s. Insets in (a-c) are the corresponding high magnification TEM images. (d) Absorption and PL emission spectra of the single chain superlattices after sonicating or stirring. (e) Optical photograph of the 1D self-assembled superlattice structures of CsPbI₃, CsPbBr₃ and CsPbCl₁.₅/Br₁.₅ NCs induced by T-PbSO₄ cluster under UV light (left to right). (f) Optical photographs of the solutions of NCs after anion exchange (I, Br, and Cl) from the self-assembled superlattices of CsPbBr₃ under UV light. CsPbI₃, CsPb(I/Br)₃, CsPb(Br/I)₃, CsPbBr₃, CsPb(Br/Cl)₃ and CsPb(Cl/Br)₃ NCs (left to right).

Upon mechanical stimulation, the pea-pod architecture can be further transformed into a structure in which all of the CsPbBr₃ NCs are expelled out of the half-cylindrical casings. TEM (Fig. 4a) and SEM (Fig. S8) images of the single chain superlattice samples subjected to sonication for 30 s in hexane clearly show that the cubic NCs uniformly relocated from the center of the shells to a bound state along the edges of the casings. This process is not reversible, even under prolonged sonication for 30 minutes (Fig. 4b). This inside-out transformation was also observed in a separate experiment where the pea-pod structures were subjected to magnetic stirring for 30 s (Fig. 4c), confirming that the pea-pod inclusion complex is a metastable, kinetic product that transforms into a more stable complex upon the input of mechanical energy. Additionally, the corresponding absorption and emission spectra of inside-out transformation exhibit no shift, despite their distinct shapes (Fig. 4d). The thermodynamic stability of the along-side assembly product may arise from entropy gains from uncurving the nanoribbon hosts as well as extra stabilization from NCs-PbSO₄ cluster through hydrophobic ligands interactions. The irreversible switching between different self-assembled hierarchical structures verifies that the self-assembly process can be delicate, often driven by weak interactions,[9, 19, 34]

Different assemblies of PbSO₄-perovskite NCs can be realized by manipulating either the solvents or the mechanical input, which favors different kinetically trapped products. The kinetic assembly product, the pea-pod like nanostructures, involved curving of the ribbon-like template into half cyclindrical shells around a 1D chain of CsPbBr₃ NCs. This induced-fit shell transformation and the 1D chain assembly, both being energetically expensive, may be compensated by the favorable NCs-cluster interactions as well as cooperative interparticle packing, driven by a fine balance between solvophobic and solvophilic interactions.[34] The formation of multi-line assemblies by using smaller particles indicates that the system is accommodating towards a tight-fit "host-guest" system. The irreversible transformation into the along-side assembly suggests that the mechanical energy input easily overcomes the kinetic barrier for the formation of the more thermodynamically stable product.

### Anion Exchange

We have also studied the impact of using CsPbX₃ NCs with different halide compositions for 1D chain assembly. [26, 42] TEM images confirm the well-defined lines of close-packed 1D superlattice structures are formed when CsPbI₃ (diameter: 12.4 nm) and CsPbCl₁.₅/Br₁.₅ (diameter: 9.5 nm) are used for self-assembly (Fig. S9). The optical photographs of the 1D self-assembled superlattice structures of CsPbI₃, CsPbBr₃ and CsPbCl₁.₅/Br₁.₅ NCs display bright red, green and cyan color, respectively (Fig. 4e). Post assembly anion-exchange is also possible, demonstrated by the tunable emission colors of the mixtures of different halide salts with pre-assembled pea-pod PbSO₄-CsPbBr₃ structures (Fig. 4f). This facile halide exchange is consistent with the formation of an open shell pea-pod nanostructures in which perovskite nanocrystals benefit from the unshielded structure.

## Conclusions

In summary, we report a detailed study of a templated self-assembly approach to achieving 1D superlattices of $CsPbX_3$ NCs. Simple mechanical stirring of the self-assembly process revealed the kinetic nature of the pea-pod like superstructures, which may transform to a more thermodynamically stable product upon sonication or agitation. This self-assembly motif is reminiscent of supramolecular host-guest systems where induced fit of the $PbSO_4$ shell and tight fit of differently sized NCs guests are observed. Overall the self-assembled superlattices are products of competitive solvophobicity and solvophilicity. Choice of a halide free solvent is vital to study the self-assembly of $CsPbX_3$ NCs. The geometric configurations of the NCs superlattices can be further controlled by adjusting the size and shape of NCs with a range of halide compositions. The general utility of this novel self-assembly process will allow the use of 1D self-assembled superlattices as a platform for both fundamental and applied research in the future.

## Conflicts of interest

There are no conflicts to declare.

## Acknowledgements

## Notes and references

1   A. P. Alivisatos, *Science,* 1996, **271**, 933.
2   M. C. Daniel and D. Astruc,  *Chem. Rev.,* 2004**, 104**, 293.
3   A. Swarnkar, R. Chulliyil, V. K. Ravi, M. Irfanullah, A. Chowdhury and A. Nag, *Angew. Chem. Int. Ed. Engl.,* 2015, **54**, 15424.
4   Y. Yin and A. P. Alivisatos, *Nature, 2005,* **437**, 664.
5   J. Ji, X. Song, J. Liu, Z. Yan, C. Huo, S. Zhang, M. Su, L. Liao, W. Wang, Z. Ni, Y. Hao and H. Zeng, *Nat. Commun.,* 2016, **7**, 13352.
6   A. Klinkova, H. Therien-Aubin, A. Ahmed, D. Nykypanchuk, R. M. Choueiri, B. Gagnon, A. Muntyanu, O. Gang, G. C. Walker and E. Kumacheva, *Nano Lett.,* 2014**, 14**, 6314.
7   L. Carbone, C. Nobile, M. D. Giorgi, F. D. Sala, G. Morello, P. Pompa, M. Hytch, E. Snoeck, A. Fiore, I. R. Franchini, M. Nadasan, A. F. Silvestre, L. Chiodo, S. Kudera, R. Cingolani, R. Krahne and L. Manna, *Nano Lett.,* 2007**, 7**, 2942.
8   B. Gao, G. Arya and A. R. Tao, *Nat. Nanotech.,* 2012, **7**, 433.
9   P. Y. Kim, J. W. Oh and J. M. Nam, *J. Am. Chem. Soc.,* 2015**, 137**, 8030.
10  L. Hu, C. Wang, R. M. Kennedy, L. D. Marks and K. R. Poeppelmeier, *Inorg. Chem.,* 2015**, 54**, 740.
11  B. Abecassis, *Chemphyschem,* 2016**, 17**, 618.
12  S. Adireddy, C. E. Carbo, Y. Yao, J. M. Vargas, L. Spinu and J. B. Wiley, *Chem. Mater.,* 2013, **25**, 3902.
13  Z. Quan, H. Xu, C. Wang, X. Wen, Y. Wang, J. Zhu, R. Li, C. J. Sheehan, Z. Wang, D. M. Smilgies, Z. Luo and J. Fang, *J. Am. Chem. Soc.,* 2014**, 136**, 1352.
14  B. Gao, M. J. Rozin and A. R. Tao, *Nanoscale,* 2013, **5**, 5677.
15  V. T. Cong, E. O. Ganbold, J. K. Saha, J. Jang, J. Min, J. Choo, S. Kim, N. W. Song, S. J. Son, S. B. Lee and S. W. Joo, *J. Am. Chem. Soc.,* 2014**, 136**, 3833.
16  J. Novak, R. Banerjee, A. Kornowski, M. Jankowski, A. Andre, H. Weller, F. Schreiber and M. Scheele, *ACS Appl. Mater. Inter.,* 2016, **8**, 22526.
17  W. R. Cai, G. Y. Zhang, K. K. Lu, H. B. Zeng, S. Cosnier, X. J. Zhang and D. Shan, *ACS Appl. Mater. Inter.*, 2017, **9**, 20904.
18  Y. Bekenstein, B. A. Koscher, S. W. Eaton, P. Yang and A. P. Alivisatos, *J. Am. Chem. Soc.,* 2015, **137**, 16008.
19  B. Gao, Y. Alvi, V. Li and A. R. Tao, *CrystEngComm,* 2014**, 16**, 9434.
20  A. Singh, A. Singh, G. K. Ong, M. R. Jones, D. Nordlund, K. Bustillo, J. Ciston, A. P. Alivisatos and D. J. Milliron, *Nano Lett.,* 2017, **17**, 3421.
21  O. Vybornyi, S. Yakunin and M. V. Kovalenko, *Nanoscale,* 2016**, 8**, 6278.
22  M. P. Arciniegas, A. Castelli, L. Ceseracciu, P. Bianchini, S. Marras, R. Brescia and L. Manna, *Nano Lett.,* 2016, **16**, 6154.
23  S. Jiang, A. Van Dyk, A. Maurice, J. Bohling, D. Fasano and S. Brownell, *Chem. Soc. Rev.,* 2017, **46,** 3792.
24  F. Biedermann and H. J. Schneider, *Chem. Rev.*, 2016, **116**, 5216.
25  H. J. Schneider, *Int. J. Mol. Sci.,* 2015, **16**, 6694.
26  G. Nedelcu, L. Protesescu, S. Yakunin, M. I. Bodnarchuk, M. J. Grotevent and M. V. Kovalenko, *Nano Lett.,* 2015, **15**, 5635.
27  L. Protesescu, S. Yakunin, M. I. Bodnarchuk, F. Krieg, R. Caputo, C. H. Hendon, R. X. Yang, A. Walsh and M. V. Kovalenko, *Nano Lett.*, 2015, **15**, 3692.
28  Z. Yuan, C. Zhou, Y. Tian, Y. Shu, J. Messier, J. C. Wang, L. J. van de Burgt, K. Kountouriotis, Y. Xin, E. Holt, K. Schanze, R. Clark, T. Siegrist and B. Ma, *Nat. Commun.,* 2017, **8**, 14051.
29  L. Luo, L. Men, Z. Liu, Y. Mudryk, X. Zhao, Y. Yao, J. M. Park, R. Shinar, J. Shinar, K. M. Ho, I. E. Perakis, J. Vela and J. Wang, *Nat. Commun.,* 2017, **8**, 15565.
30  Y. Wu, Y. Wei, Y. Huang, F. Cao, D. Yu, X. Li and H. Zeng, *Nano Res.,* 2017, **10**, 1584.
31  S. Seth and A. Samanta, *Sci. Rep.,* 2016, **6**, 37693.
32  A. Pan, B. He, X. Fan, Z. Liu, J. J. Urban, A. P. Alivisatos, L. He and Y. Liu, *ACS Nano,* 2016, **10**, 7943.
33  S. Sun, D. Yuan, Y. Xu, A. Wang and Z. Deng, *ACS Nano,* 2016, **10**, 3648.
34  X. Zhang, L. Lv, L. Ji, G. Guo, L. Liu, D. Han, B. Wang, Y. Tu, J. Hu, D. Yang and A. Dong, *J. Am. Chem. Soc.,* 2016, **138**, 3290.
35  M. J. Jurow, T. Lampe, E. Penzo, J. Kang, M. A. Koc, T. Zechel, Z. Nett, M. Brady, L. W. Wang, A. P. Alivisatos, S. Cabrini, W. Brutting and Y. Liu, *Nano Lett.,* 2017, **17**, 4534.
36  D. Parobek, Y. Dong, T. Qiao, D. Rossi and D. H. Son, *J. Am. Chem. Soc.,* 2017, **139,** 4358.
37  T. Udayabhaskararao, M. Kazes, L. Houben, H. Lin and D. Oron, *Chem. Mater.,* 2017, **29**, 1302.
38  S. Stepanow, M. Lingenfelder, A. Dmitriev, H. Spillmann, E. Delvigne, N. Lin, X. Deng, C. Cai, J. V. Barth and K. Kern, *Nat. Mater.,* 2004, **3**, 229.
39  M. D. Pluth and K. N. Raymond, *Chem. Soc. Rev.* 2007, **36**, 161.

40  Y. W. Yang, Y. L. Sun and N. Song, *Acc. Chem. Res.,* 2014, **47**, 1950.

41  L. Zhu, M. Zhu and Y. Zhao, *ChemPlusChem,* 2017, **82**, 30.

42  Q. A. Akkerman, V. D'Innocenzo, S. Accornero, A. Scarpellini, A. Petrozza, M. Prato and L. Manna, *J. Am. Chem. Soc.,* 2015**, 137**, 10276.